

<Original>

Measurement of Thermal Diffusivity of Ion-nitrided Steel by Flash Method***

Sang-Kil Lee*, Hung-Joo Lee* and Chung-Oh Lee**

(Received June 1, 1979)

섬광 열확산법에 의한 이온질화강의 열확산 계수 측정

이 상 길 · 이 흥 주 · 이 정 오

초 록

이온 질화강 확산층의 열확산 계수를 섬광열 확산 계수측정법에 의하여 실험적으로 구하였다. 섬광 열확산 계수 측정법은 둥근 원판모양의 얇은 시편전면에 순간적으로 강렬한 열을 가하여 확산시킨후 후면에서 증가되는 온도를 기록하여 컴퓨터에 의한 데이터 소거법을 이용해서 열확산 계수를 측정하는 것이다.

본 연구에서는 섬광 열 확산 계수 측정법에 의하여 지극히 얇은 재료의 열확산 계수를 측정 할 수 있음을 입증하였으며, 구조용 재료가 상온에서 갖는 열 확산 계수를 이온질화 처리를 하지 않았을 경우와 이온질화 처리를 하였을 경우의 두가지로 나누어 측정하였다. 위의 실험결과로부터 이온질화처리를 실시하면 약 10%까지 열확산 계수가 증가하는 것을 발견하였다.

Nomenclature

English Letter Symbols

- C Specific heat at constant pressure ($Jg^{-1} K^{-1}$)
- K Thermal conductivity ($W cm^{-1} K^{-1}$)
- l Sample thickness (cm)
- r Pulse shape parameter
- R $y_{1/2}/t_p^2$
- Q_0 Adjustable parameter
- $Q(t)$ Heat pulse function
- q_0 Total energy absorbed by unit area of the surface
- $q(t)$ Rate of energy absorption per unit area

- t Time variable (sec)
- t_p Pulse peak time (sec)
- $T(z,t)$ Temperature in the slab at location Z and time t ($^{\circ}C$)
- T_0 Initial temperature ($^{\circ}C$)
- v Voltage (Volt)
- V Normalized temperature excursion
- x Adjustable parameter
- y Heat diffusion time (sec)
- z Z-direction

Greek Letter Symbols

- α Thermal diffusivity (cm^2/sec)
- $\theta(z,t)$ Temperature rise caused by heat pulse($^{\circ}C$)
- $\theta(z,s)$ Laplace transform of (z,t)
- θ Final adiabatic temperature difference ($^{\circ}C$)
- ρ Density (g/cm^3)
- τ Pulse time of xenon flash tube (sec)

* Member, Dept. of Ord. Eng., Korea Military Academy.

** Member, Dept. of Mech. Eng., KAIS.

*** Presented at the KSME Spring Conference, Chun-Ju, May 26, 1979.

I. Introduction

In order to satisfy the real needs of industry using various steels, an ion nitriding [1, 2, 3, 4] surface treatment on steel is most important because of its enhancing material properties in wear, erosion, and corrosion resistance protection. It is then an important and interesting problem to predict and measure the thermophysical properties including thermal conductivity and thermal diffusivity. In this work, the thermal diffusivity of ion-nitrided steel is measured by a flash method.

In the flash method for measuring the thermal diffusivity [5, 6, 7, 8, 9, 10], a high intensity-short-duration heat pulse of radiant energy from an optical flash lamp or laser is used to irradiate one of the two flat parallel surface of a homogeneous sample and the subsequent history at the opposite surface is monitored with a thermocouple or a photomultiplier tube. The pulse raises the average temperature of the sample only a few degree above its initial value. The thermal diffusivity of the sample material may then be deduced from the shape of the resulting temperature transient if the heat diffusion equation has been solved for the particular boundary conditions of the experiment. In the simplest form of the experiment, it is assumed that heat flow is one dimensional, that material properties are temperature independent and that the heat pulse is uniform over the sample surface [5, 6, 7, 8, 9, 10].

The effect of non-instantaneous heat pulse on the shape of the rear-face transient is important. Cape and Lehman [8] have shown that this transient is retarded with pulses of finite duration, referring the retardation as the "finite pulse time effect" [11, 12, 12, 14]. Larson and Koyama [11] have shown that one can completely eliminate those errors due to the finite pulse time effect even for samples as thin as $l = (\alpha\tau)^{1/2}$ by applying an empirical function which more closely describes the pulse shape. Here l is the thickness of the sample, α is the thermal

diffusivity, and τ is the time in seconds representing the duration of the heat pulse. The thickness of the disk-shaped samples used in the experiment is less than $4(\alpha\tau)^{1/2}$. The samples are made of the homogeneous diffusion layer of a ion-nitrided steel.

II. Mathematical Analysis

In the usual flash technique, the front surface of the homogeneous sample is subjected to a heat pulse and the resulting temperature rise of the rear surface is recorded.

From this temperature rise, the thermal diffusivity of the material is obtained by the computer data reduction with mathematical analysis [11].

A realistic empirical function of the heat pulse may be derived as follows. It has been found that the representation of the pulse shape for the xenon flash tube employed in the experiments is afforded by a function of the form,

$$Q(t) = (Q_0 t) \exp(-xt), \quad t > 0 \quad (1)$$

where Q_0 and x are adjustable parameters, and t is the time in seconds. The response of a photodiode detector to a typical pulse from the xenon flash tube is shown in Figure. By setting $\dot{Q}(t=t_p) = 0$

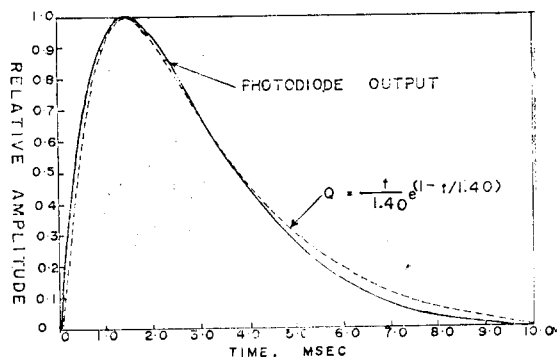


Fig. 1. Response of the photodiode detector to a pulse from xenon flash tube; dashed line represent functional approximation to the pulse shape.

in equation (1), where dot indicates time differentiation and t_p is the pulse peak time μ_s determined from an oscilloscope trace of the photodiode output,

we get $x=1/t_p$. Hence, equation (1) becomes

$$Q(t) = (Q_0 t) \exp(-t/t_p), \quad t > 0. \quad (2)$$

In order to compare equation (1) with actual flash tube behaviour, $Q(t)$ may be normalized to unity at the maximum of the oscilloscope trace. Thus $Q_0 = \exp(1/t_p)$, and equation (2) becomes

$$Q(t) = (t/t_p) \exp(1-t/t_p), \quad t > 0 \quad (3)$$

The equation(3) is plotted in Figure 1.

It may be seen that this function satisfactorily represents the pulse shape. The rate of energy absorption may therefore be represented by

$$q(t) = (bt) \exp(-t/t_p), \quad t > 0, \quad (4)$$

where, $q(t)$ is the rate of energy absorption per unit area at the front face and b is a constant by the requirement

$$\int_0^{\infty} q(t) dt = q_0.$$

Here, q_0 is the total energy absorbed by unit area of the surface. The above requirement leads to $b = q_0/t_p^2$, so that equation(4) for the heat pulse function becomes

$$q(t) = (q_0/t_p^2) t \exp(-t/t_p), \quad t > 0. \quad (5)$$

To solve the heat diffusion equation with the appropriate boundary conditions, the following assumptions are made :

- (1) Heat flow is one dimensional.
- (2) There is no heat loss from the sample surfaces.
- (3) Heat pulse is uniformly absorbed on the front surface.

An appropriate model corresponding to these assumptions takes the form of slab of infinite extent in the radial direction, with the parallel and planar front and rear surface at $z=0$ and $z=l$, respectively.

At time $t=0$, when the slab is at temperature T_0 , the front surface is uniformly irradiated by a flash tube, which results in energy absorption of the sample with temporal behaviour described by equation(5). The subsequent temperature history is recorded at the rear surface. With these assumptions heat flow in the sample is described as follows,

$$-k\theta_{zz}(z,t) + PC\theta_t(z,t) = 0, \quad 0 < z < l, \quad t > 0, \quad (6)$$

$$\theta(0 < z < l, t = 0_+) = 0, \quad (7)$$

$$-k\theta_z(z=0, t > 0) = (q_0/t_p^2) t \exp(-t/t_p), \quad (8)$$

and

$$\theta_z(z=l, t > 0) = 0. \quad (9)$$

Here ρ is density, C is heat capacity, and K is thermal conductivity. In equations (6) through (9), the temperature excursion is denoted by $\theta(z,t) = T(z,t) - T_0$, where $T(z,t)$ is the temperature in the slab at location Z and at time t . Differentiation is indicated by the notation $\theta_z = \partial\theta/\partial z$,

$$\theta_{zz} = \partial^2\theta/\partial z^2.$$

By using Laplace transformation, the following transformed solution is obtained.

$$\theta(z,s) = \frac{H \operatorname{Hcosh}(ns^{1/2})}{S^{1/2} \cdot \sinh(y^{1/2} \cdot s^{1/2}) (s + \frac{1}{t_p})^2}, \quad (10)$$

where

$$H = (q_0/t_p^2) / (K\rho C)^{1/2}, \quad (10-1)$$

$$n = y^{1/2}(1-z/l), \quad (10-2)$$

and

$$y = l^2/\alpha. \quad (10-3)$$

Here y is the heat diffusion time in sec.

The expression for the temperature excursion is given by the inversion integral [15] as

$$\theta(z,t) = \frac{H}{2\pi i} \int_{x_0-i\infty}^{x_0+i\infty} \frac{e^{st} \operatorname{cosh}(ns^{1/2})}{S^{1/2} \cdot \sinh(y^{1/2} \cdot s^{1/2}) (s + \frac{1}{t_p})^2} ds,$$

$$0 < z < l. \quad (11)$$

Taking the temperature excursion relative to the final adiabatic equilibrium temperature difference θ_{∞} , a dimensionless variable $W(z,t)$ is defined as follows.

$$W(z,t) = \theta(z,t) / \theta_{\infty}, \quad (12)$$

where

$$\theta_{\infty} = T(t \rightarrow \infty) - T_0 = q_0/\rho Cl$$

Dividing both sides of equation(11) by θ_{∞} , the following expression for $W(z,t)$ is obtained.

$$W(z,t) = \frac{R}{2\pi i} \int_{x_0-i\infty}^{x_0+i\infty} g(s) ds, \quad 0 < z < l, \quad (13)$$

where, the integrand $g(s)$ is given by

$$g(s) = \frac{e^{st} \operatorname{cosh}(ns^{1/2})}{S^{1/2} \sinh(y^{1/2} \cdot s^{1/2}) (s + \frac{1}{t_p})^2}, \quad (14)$$

and

$$R = y^{1/2}/t_p.$$

The integrand $f(s)$ of equation (14) has the following singularities:

a branch point at $s=0$,

a pole at $s=-1/t_p$,

and an infinite row of simple poles S_k along the negative real axis of the complex S plane corresponding to the zeros of $\sinh(y^{1/2} \cdot s^{1/2})$. A contour consisting of the closed circuit ABDOEA, appropriate to the above inversion, is given in Figure 2. On and within this closed contour, the integrand $g(s)$ is analytic and single-valued since the contour encloses no singularities. Hence by cauchy's integral theorem [16] one obtains

$$\int g(s)ds = \left[\int_{AB} + \int_{C_R} + \int_{DOE} \right] g(s)ds = 0. \quad (15)$$

using equation (13) and equation(14), the following expression is obtained.

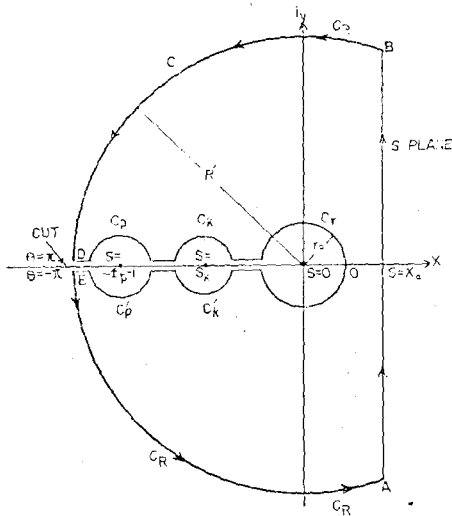


Fig. 2. Contour for the inversion of equation (11); Laplace transform on the temperature excursion function.

From Figure 2,

$$W(z,t) = \frac{R}{2\pi i} \lim_{R \rightarrow \infty} \int_{EOD} g(s)ds. \quad (16)$$

Line integral on C_r around branch point $s=0$;

$$\int_{C_r} g(s)ds = 2\pi i/R \quad (17)$$

Line integral around the poles $S=S_k$;

$$2\sum_{k=1}^{\infty} \int_{C_k} g(s)ds = \frac{4\pi i r^2}{R} \sum_{k=1}^{\infty} (-1)^k \frac{\exp(-k^2\pi^2 t/y) \cos(k\pi(1-z/l))}{(r-k^2\pi^2)^2} \quad (18)$$

where

$$r = y/t_p = l^2/at_p \neq k^2\pi^2, \quad k=1, 2, \dots$$

Line integral around pole $s = -\frac{1}{t_p}$;

$$2 \int_{C_p} g(s)ds = -\frac{\pi i r^{1/2} \cdot \exp(-t/t_p) \cos(n/t_p^{1/2})}{R \cdot \text{Sin}(r\frac{1}{2})} \times \left[1 + 2\frac{t}{t_p} + r^{1/2} \cot r^{1/2} + \frac{n}{t_p^{1/2}} \cdot \tan\left(\frac{n}{t_p^{1/2}}\right) \right] \quad (19)$$

Expression for the temperature excursion;

$$\lim_{R \rightarrow \infty} \int_{EOD} g(s)ds = \left[\int_{C_r} + 2\sum_{k=1}^{\infty} \int_{C_R} + 2 \int_{C_P} \right] g(s)ds \quad (20)$$

Thus the following expression can be obtained for the dimensionless temperature excursion by combining equation (16), (17), (18), (19) and (20):

$$W(z,t) = 1 + 2r^2 \sum_{k=1}^{\infty} (-1)^k \frac{\exp(-k^2\pi^2 t/y) \cos(k\pi y^{-1/2} n)}{(r-k^2\pi^2)^2} - \frac{r^{1/2} \exp(-t/t_p) \cos(t_p^{-1/2} n)}{2 \cdot \text{Sin} r\frac{1}{2}} \left[1 + 2\frac{t}{t_p} + r^{1/2} \cot r^{1/2} + n/t_p^{1/2} \cdot \tan\left(\frac{n}{t_p^{1/2}}\right) \right] \quad (21)$$

Equation (21) becomes, by setting $Z=l$,

$$V(t:y,t_p) = 1 + 2r^2 \sum_{k=1}^{\infty} (-1)^k \frac{\exp(-k^2\pi^2 t/y)}{(r-k^2\pi^2)^2} - \frac{r^{1/2} \cdot \exp(-t/t_p)}{2 \cdot \text{sin} r\frac{1}{2}} (1 + 2\frac{t}{t_p} + r\frac{1}{2} \cot r^{1/2}), \quad (22)$$

where V has the usual definition

$$V(t) = \frac{\theta(z=l,t)}{\theta_{\infty}} = \frac{T(x=l,t) - T_0}{T(t \rightarrow \infty) - T_0}$$

Equation (22) is used to compute thermal diffusivity.

III. Experimental Procedure

The flash method is shown schematically in Figure 3 using a flash lamp as the energy source and an oscilloscope trace as the recording device.

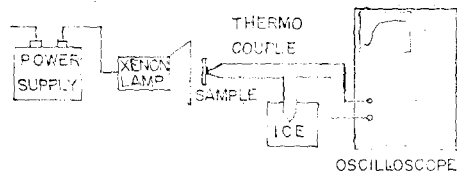


Fig. 3. Outline of flash diffusivity apparatus.

The success of the flash technique depends upon adequately meeting the boundary conditions of theory. The front surface of the sample must be uniformly irradiated. The thermocouple must measure the actual rear surface temperature, and heat losses must be minimized. Furthermore, the signal must be large enough to be well above the noise level in the recording system, and the bandwidth of the amplifier and recorder must be wide enough to pass the signal without disturbances.

The xenon flash tube used in the experiment is a commercially available unit (IL LI IND. CO. LTD. SS-1200) consisting of a ring type quartz tube dissipating 400 joules of energy in each flash.

In the present experiment, the reflecting mirror which is made of aluminum foil was attached in order to improve irradiation effect. The front face of the sample were uniformly blackend with camphor black to increase the amount of energy absorbed. These samples were mounted in a sample holder at a short distance (less than 5cm) from the flash tube. The front surface of the samples were parallel to the axis of the xenon flash quartz tube and the back surface of them was welded with a chromel Alumel thermocouple wire with 0.1mm diameter. The thermocouple wires were junctioned at the center of the rear surface of the samples for reducing the disturbing effects caused by heat loss at the edge of the samples.

The output voltage from the thermocouple was shown on a storage oscilloscope (Tektronix 7603) and photographed with a polaroid land camera. The maximum voltage was usually 200 to 320 μ volts indicating rear surface temperature rise of 5° to 8°C.

The sample holders must be opaque to prevent irradiation of the back surface of the sample. In order to reduce the heat transfer from the sample to the sample holder by conduction, the contact area is minimized. The sample thickness should also be minimized for preventing the convective heat transfer at the edge of the sample.

Instantaneous spark at the beginning of triggering

is caused by 1.5 volt trigger pulse, but the spark did not influence the output signal on the oscilloscope, since the trigger pulse was disappeared immediately.

The temperature rise curve on the rear surface of samples near room temperature is shown in Figure 4. As shown in Figure 4, the signal reached the sharp peak point at the beginning because of trigger pulse, but rapidly comes back to the base line and then rises slowly to the maximum point.

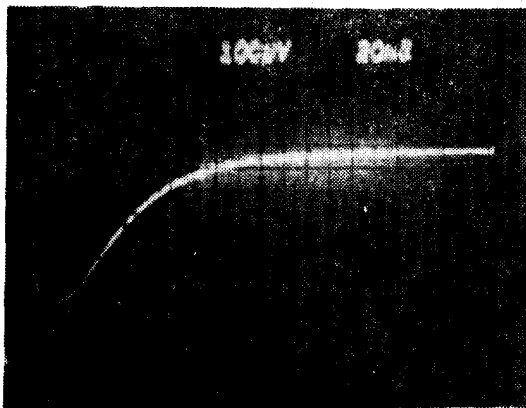


Fig. 4. Polaroid land print of the oscilloscope display of the detector output.

If the final temperature is reached very slowly after an initially fast rise, it may indicate non-uniform heating on the front surface. If the signal gradually increases to the maximum temperature from the beginning to the end, it also represents the heat loss from the sample surfaces.

It is necessary to find the peak time (time to reach the maximum intensity) of heat pulse to obtain a better experimental results. The empirical function for the heat pulse can be represented as follows,

$$Q(t) = (t/t_p) \exp(1-t/t_p): t > 0,$$

where $Q(t)$ is an empirical intensity function of the heat pulse, t is a time in seconds, and t_p is the time to reach the maximum intensity.

In the present experiment, a Korea photoelectronics sp-1KL planar type silicon photodiode was used. The photodiode detector has a peak spectral response at 0.8 μ wavelength and has substantial

sensitivity in the infra-red region. The circuit diagram of photodiode detector is shown in Figure 5.

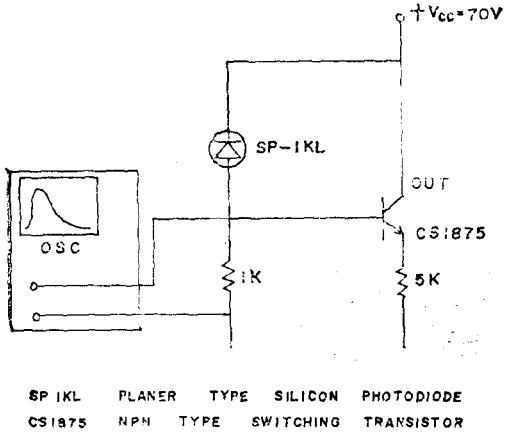


Fig. 5. The circuit of photodiode detector

The oscilloscope trace of the photodiode output for the xenon flash tube is shown in Figure 6.

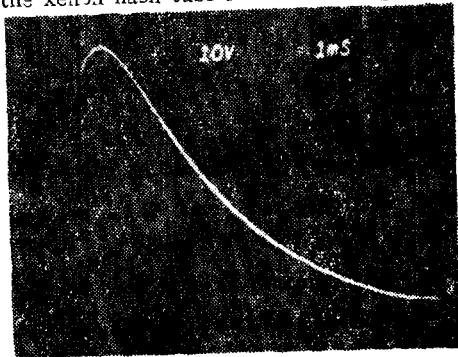


Fig. 6. Photodiode output of the Xenon flash tube.

From the Figure 6, the peak time t_p , can be easily determined as 1.4 milliseconds.

IV. Discussions and Conclusions

It has been known that the nitrided material would have the various compound and diffusion layer according to the nitriding conditions. The thickness of samples was determined according to the nitrided layer to make a homogeneous sample. The samples were wholly nitrided along the axial direction. The compound layer was ground off to make a homogeneous sample.

The metallographic structures of the non-nitrided sample is shown in Figure 7. The microscopic

structures of a sample made of SCM 3 steel can be compared with the compound and diffusion layer in an ion-nitrided SCM 3 steel in the Figure 8 and 9.

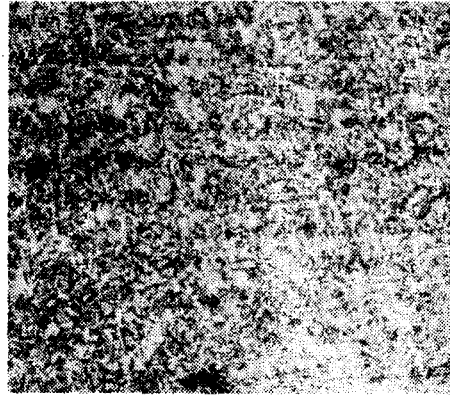


Fig. 7. Metallographic view of SCM 3.

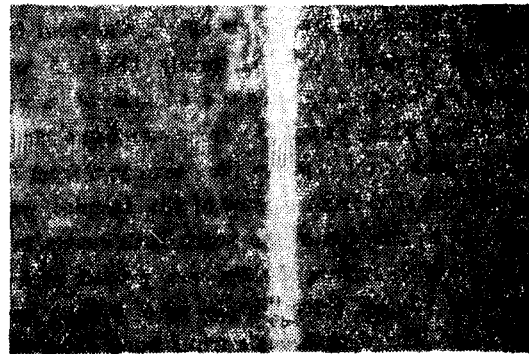


Fig. 8. Metallographic view of ion-nitrided steel (diffusion layer (a)+compound layer (b)) SCM 3;5 torr, 550°C, 6hrs (400x).

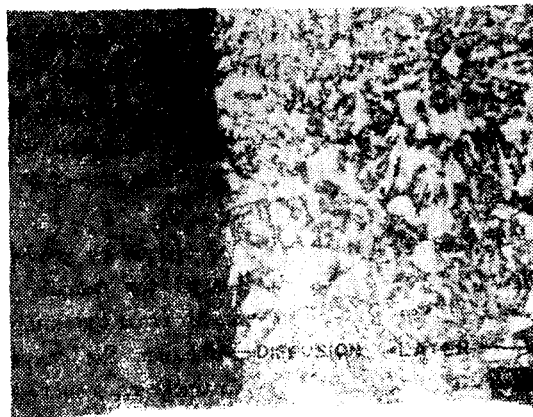


Fig. 9. Metallographic view of ion-nitrided steel (diffusion layer) SCM 3;5 torr, 550°C, 12hrs (400x).

Theoretical temperature rise with a constant value of α fits the experimental temperature rise very well as shown in Fig. 10.

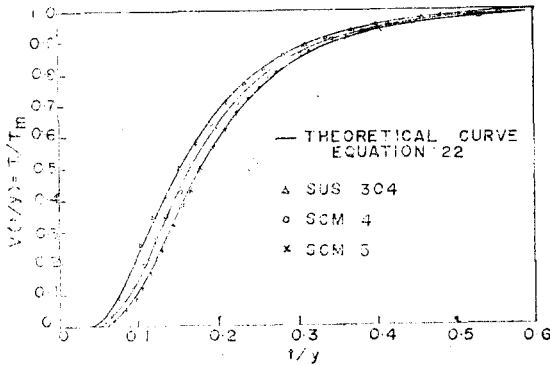


Fig. 10. Theoretical rear face transients and experimental oscilloscope trace points for various samples.

Therefore it may be concluded that influence tending to distort the shape of the experimental temporal transient away from theoretical shape is almost negligible. The experimental results of the thermal diffusivity of non-nitrided steels and ion-nitrided steels at 22°C are listed in table I and table II one another.

Table I. Thermal Diffusivity of Steels Before Ion-Nitriding.

Sample		L	Dia.	t1/2	α at 22°C	α (other sources)
JIS No.	AISI No.	(cm)	(cm)	(msec)	(cm ² /sec)	(cm ² /sec)
SOM 2	AISI 4130	0.0375	1.975	14	0.0936	
SCM 3	AISI 4135	0.0989	1.535	17	0.0947	
SCM 4	AISI 4140	0.0990	1.489	18.5	0.0873	
SCM 5	AISI 4145	0.0795	1.500	13.1	0.0864	
SCM 22		0.085	1.510	13.8	0.0850	
SNM 8	AISI 4340	0.0307	2.000	13.8	0.0373	0.091b (17)
UUS 304	AISI 304	0.0950	1.500	38	0.0356	0.035c (18)

a. obtained from Eq. (22)

b. from reference (17)

c. taken from reference (18)

Table II. Thermal Diffusivity of Ion-Nitrided Steels

Sample		L(cm)	Dia.(cm)	t1/2 (msec)	α at 22°C (cm ² /sec)
JIS No.	AISI Mo.				
SCM 2	AISI 4130	0.0955	2.000	15.6	0.100
SCM 3	AISI 4135	0.0985	1.535	16.8	0.0970
SCM 4	AISI 4140	0.099	1.490	16.5	0.100
SCM 5	AISI 4145	0.0785	1.500	11.9	0.0956
SCM 22		0.080	1.470	17.8	0.0931
SNM 8	AISI 4340	0.0975	2.010	17.5	0.0890

Deviation of experimental data from the theoretical shape may come from the disturbances by noise signal and non-uniform absorbing of heat pulse at the front surfaces of samples. The experimental apparatus for measuring thermal diffusivity was designed to minimize all of the disturbances and careful calibration was performed. Therefore the maximum differences caused in the diffusivity measurement were within 5% to the reported value.

From this study, we may draw the following conclusions.

- (1) The thermal diffusivity of ion nitrided steels can be measured by flash method.
- (2) Thermal diffusivity of the steels is increased up to 10% by the ion nitriding surface treatment.

List of References

1. American Society for Metals, *Metals Hand book*, 8th Edition, Vol. 2, pp. 149. 1964.
2. H.Bennek, O.Rudiger, Arch für Eisen Hult, 18 (10), 1944
3. C.T. Jones, S.W. Martin, D.J. Struges, and M. Hudis, "Ion Nitriding", pp. 72, Metal progress, 1972.
4. 山中久彦: イオン窒化法, p.24 日刊工業新聞社 1976
5. W.J. Parker, et. al., "Flash Method of Determining Thermal Diffusivity, Heat Capacity, and Thermal Conductivity", *J. Appl. phys.* 32. 1679 (1961).
6. R.L. Rudkin, R.J. Jenkins, and W.J. Parker,

- "Thermal Diffusivity Measurements on Metals at High Temperatures", *Rev. Sci. Instr.* 33, 21, (1963).
7. R.D. Cowan, "Pulse Method of Measuring Thermal Diffusivity", *J. Appl. Phys.* 34, 926 (1963).
 8. J.A. Cape and G.W. Lehman, "Temperature and Finite pulse time Effects in the Flash Method for Measuring Thermal Diffusivity", *J. Appl. Phys.* 34, 1909, (1963).
 9. H.W. Deem and W.D. Wood, "Flash Thermal Diffusivity Measurement Using a Laser", *Rev. Sci. Instr.* 33, 1107 (1962).
 10. R.J. Jenkins and W.J. Parker, "A Flash Method for Determining Thermal Diffusivity Over a wide Temperature Range", U.S. Naval and Radiological Defense Laboratory, *WADD Technical Report*, 61—95.
 11. K.B. Larson and Karl Koyama, "Correction for Finite Pulse Time Effects in Very Thin Samples Using the Flash Method of Measuring Thermal Diffusivity", *J. Appl. Phys.* 32 (9), 1679—84, 1960.
 12. R.C. Heckman, "Finite Pulse Time and Heat Loss in Pulse Thermal Effects in Pulse Thermal Diffusivity Measurements", *J. Appl. Phys.* 44 (4), 1415—1460, 1973.
 13. R.E. Taylor, J.A. Cape, "Finite Pulse Time Effects in the Flash Diffusivity Technique", *Appl. Phys. Lett.*, 5, 212—13, 1964.
 14. D.A. Watt, "Theory of Thermal Diffusivity by Pulse Technique", *British J. Appl. Phys.*, 17, 231—40, 1966.
 15. H.S. Carslow, J.C. Jaeger, *Conduction of Heat in Solids*, Oxford University Press, 2nd Edition, 302, 1959.
 16. F.B. Hildebrand, "Advanced Calculus for Engineers", Chap. 10, p 524, Prentice-Hall, Inc., New York, 1949.
 17. C.P. Buttler and E.C.Y. Inn in *Thermodynamic and Transport Properties of Gases, Liquids and Solids* (American Society of Mechanical Engineers, 29 w. 39th st. New York, 1959.)
 18. R.J. Jenkins and Westover. R.W., "The Thermal Diffusivity of Stainless Steel over the Temperature Range 120°C to 1000°C" UNSRDL-TR-484, 1-13, 1960. (AD 249578).
-